Modified Zeroing Neurodynamics Models for Range-Based WSN Localization From AOA and TDOA Measurements

Lijuan Wang, Dan Su, Mei Liu, and Xiujuan Du

***Abstract*—With the rise of the internet of things, wireless sensor network (WSN) technology has gained unprecedented development and has attracted increasing attention from researchers. Due to the inherent characteristics of WSN, such as interaction with the environment, WSN localization becomes an essential and attractive topic in academia and industry. In this paper, the range-based localization problem in a mobile WSN application scenario is considered to be time-varying and modeled as a dynamic matrix equation by introducing the time parameter. Two modified zeroing neurodynamics (ZND) models are proposed and investigated to deal with range-based WSN localization problems from angle of arrival (AOA) measurement and time difference of arrival (TDOA) measurement. In addition, the convergence of the proposed models is theoretically analyzed. Furthermore, computer simulations on WSN localization are carried out to prove the effectiveness of the proposed models in terms of accuracy and robustness to the dynamic environment. Additionally, the application to underwater sensor node localization of underwater acoustic network (UAN) testbed is provided to illustrate the feasibilities of the proposed models for solving UAN localization problem.**

***Index Terms*— Angle of arrival, time difference of arrival, wireless sensor network localization, zeroing neurodynamics model.**

I. Introduction

LOCALIZATION technology is widely used in natural and artificial systems. Typical examples include echolocation systems of animals [1], migration habits of birds [2], wireless sensor networks (WSNs) [3], satellite networks [4], etc. Location-based services play an essential role in people's daily life. For instance, wise healthcare can monitor the physiological state of nursing targets and locate their positions in case of an emergency; in a retail venue, with the help of tracking the personnel location, salespersons prepare customer preferences when they receive a notification of customer entry. These scenarios are implemented in WSN and supported by accurate localization solutions. Therefore, localization technology is vital for WSN applications that are particularly sensitive to location information [5].

WSN is a data-centric network, in which sensing data is collected by randomly distributed sensor nodes, usually bound to sensor positions, and finally transmitted to a remote application [6]. In general, the sensor position is obtained through physical hardware measurement or algorithm estimation [7]. Considering cost efficiency, a few powerful sensor nodes in WSN, called anchor nodes, are equipped with global positioning system (GPS) modules or deployed at predetermined positions to obtain their own positions in advance. Other sensor nodes that are not aware of their positions are called unknown nodes. They need to estimate their positions by localization solutions with the assistance of anchor nodes.

Many localization solutions for WSNs have been investigated to provide the position information of unknown nodes, e.g., range-based and range-free [8]. Owing to range esti-

Manuscript received February 14, 2022; revised May 9, 2022; accepted May 18, 2022. Date of publication May 30, 2022; date of current version July 1, 2022. This work was supported in part by the National Natural Science Foundation of China under Grant 61962052 and in part by the Innovation Team Foundation of Qinghai Office of Science and Technology under Grant 2020-ZJ-903. The associate editor coordinating the review of this article and approving it for publication was Prof. Stefan Knauth. *(Corresponding author: Xiujuan Du.)*

Lijuan Wang is with the Department of Computer, Qinghai Normal University, Xining 810008, China (e-mail: 1041517271@qq.com).

Dan Su and Mei Liu are with the School of Information Science and Engineering, Lanzhou University, Lanzhou 730000, China (e-mail: sud20@lzu.deu.cn; liumeisysu@qq.com).

Xiujuan Du is with the Qinghai Provincial Key Laboratory of IoT, the State Key Laboratory of Tibetan Intelligent Information Processing and Application, the Academy of Plateau Science and Sustainability, and the Department of Computer, Qinghai Normal University, Xining 810008, China (e-mail: dxj@qhnu.edu.cn).

Digital Object Identifier 10.1109/JSEN.2022.3177409

mates or angle estimates by additional hardware, range-based solutions generally have a higher localization accuracy as compared to range-free solutions. In this paper, a neurodynamics method is provided for solving the range-based WSN localization problem. Specifically, two modified zeroing neurodynamics (ZND) models along with different activation functions (AFs) designed for the angle of arrival-based and time difference of arrival-based WSN localization problems are proposed. Analytical discussions and computer simulations show that the modified ZND models are applied to WSN localization with satisfactory convergence, high accuracy, and robustness to the dynamic environment. Additionally, a comparative simulation of the modified ZND models with the multidimensional Kalman Filter (KF) algorithm in the example of locating the vehicle is performed to demonstrate the effectiveness of the modified ZND models.

The remainder of this paper is organized as follows. Section II reviews the work related to localization solutions of sensor nodes. Section III is intended as an introduction to the WSN localization problem modeling. The modified ZND models are proposed in Section IV, together with the analytical discussions on the convergence. In Section V, computer simulations on WSN localization and underwater acoustic network (UAN) localization are carried out. Section VI concludes this paper. The main contributions made by this paper are pointed out as below.

1) Neurodynamics methodology is explored and extended to the WSN. To be specific, modified ZND models are proposed to solve the range-based WSN localization problem efficiently.
2) The range-based localization problem from angle of arrival (AOA) or time difference of arrival (TDOA) measurement in a mobile WSN application scenario is considered to be time-varying and modeled as a dynamic matrix equation.
3) Two modified ZND models with different AFs are proposed to solve the aforementioned range-based WSN localization problems. Moreover, analytical discussions and computer simulations verify the effectiveness of the modified ZND models with high accuracy and robustness to the dynamic environment.

Notations: To lay a basis for further investigation, parameter settings and definitions employed in the ensuing sections are listed in TABLE I.

TABLE I
SUMMARY OF NOTATIONS AND DESCRIPTIONS

$+$	The pseudoinverse operator
$^{\mathrm{T}}$	The transpose operator
$\mathrm{sgn}\{\cdot\}$	The sign function
$\|\|\cdot\|\|_2$	The Euclidean norm
$T_i(t)$	The time of signal from the unknown node to the ith anchor node
$\Delta T_{i1}(t)$	The time difference of signal from the unknown node separately to the ith and first anchor nodes
$r_i(t)$	The distance between the unknown node and the ith anchor node
$r_{i1}(t)$	The distance difference from the unknown node to the ith and first anchor nodes
$\alpha_i(t)$	The arrival angle of the communication signal between unknown node and the ith anchor node
$\vec{a}$	The acceleration of the vehicle
x_k	The X-coordinate at k moment
v_k^x	The velocity in X direction at k moment
y_k	The Y-coordinate at k moment
v_k^y	The velocity in Y direction at k moment
$\Delta T(t)$	The sampling interval
Q	The covariance matrix of the process noise
R	The covariance matrix of the measurement noise
A	The state transition matrix
B	The control matrix
H	The measurement matrix
P	The covariance matrix of the state

II. RELATED WORK

In this section, we mainly review the work related to localization solutions of sensor nodes.

Existing localization solutions can be broadly classified into the following categories: distributed and centralized, range-free and range-based, anchor-based and anchor-free. Specifically, for centralized localization solutions, there is a central node being responsible to aggregate the localizing information and calculate the positions of other nodes. On the contrary, each node determines its own position in distributed solutions. In [5], a novel intelligent localization algorithm is investigated to enable each sensor node determine its own position by passively listening to the beacon signals. Although providing good accuracy, it requires the beacon node to vary the transmitted power at each transmission. In [6], a series of centralized and distributed expectation-conditional maximization algorithms based on distance measurements are developed to approximate the maximum likelihood estimator of the unknown positions. They can provide good performance even working without the prior knowledge of the measurement error statistics.

Furthermore, range-based solutions are supported by one or two range measurement techniques that measure specific physical properties of communication signals (for example, received signal strength (RSS), angle of arrival (AOA), time of arrival (TOA), and time difference of arrival (TDOA)) to achieve range measurements between the unknown node and anchor nodes. Subsequently, utilizing measured range information, range-based solutions conduct the geometric calculation and work out the position of the unknown node by establishing the system of equations to accomplish the localization process. While, range-free localization solutions estimate the positions of sensor nodes using connectivity information between sensor nodes rather than ranging (i.e., distance or angle) information. Authors in [9] present a path mechanism for beacon-assisted localization in WSN to increase the accuracy of the estimated position. Obstacle are taken into account in the design of an efficient localization approach [10] for WSN to improve localization accuracy in a realistic environment. The mobility information of sensors is utilized in two range-based models, namely the TOA model and the RSS model, to achieve node localization [11]. In view of energy efficiency, Kan *et al.* [12] provide a location and tracing system for WSNs to achieve highly accurate tracking of targets. Although such two technologies improve the energy efficiency of the system, they also increases the complexity and uncertainty of the system.

Actually, the localization problem in a mobile WSN application scenario is investigated in these literature, where the positions of nodes vary over time. In this regard, the WSN localization problem can be considered time-varying. However, as in [9]–[12], most existing works deal with this problem in a static manner. Besides, the abilities of existing works are limited when solving the time-varying WSN localization problem due to the use of static methods. Considering the fact that range-based solutions generally have a higher localization accuracy as compared to range-free solutions, they are suitable for WSN applications that demand high-precision position information [13], [14]. Consequently, in this paper, the time-varying WSN localization problem is modeled as a dynamic matrix equation by introducing the time parameter. Based on AOA and TDOA measurement algorithms, the neurodynamics method is provided for solving the time-varying WSN localization problem to achieve fast and accurate localization. Notably, the neurodynamics method we provide is used for the geometric calculation after acquiring range information.

Up to now, a number of powerful and intelligent technologies have been applied in WSNs to solve various problems effectively, for instance, multi-agent based distributed artificial intelligence for power allocation [15], conventional neural networks for secure routing [16], the firefly algorithm for dynamic cluster formation [17], and so on. Beyond that, neural networks [18]–[21] are also well extended and applied to WSNs. Thereinto, zeroing neural network (ZNN) proposed in [22], as well as its modifications [23]–[27], show their superior efficiency and accuracy for handling some complex academic and practical problems, such as the time-variant Sylvester equation solving [28], [29], nonlinear optimization [30], [31], and automatic control [32]. Furthermore, some methods based on ZNN have recently been reported and adopted to deal with wireless localization problems. In [28], a noise-suppressing model for solving time-variant generalized Sylvester equations is presented. Its application to acoustic source localization illustrates the ability of this model in localizing a moving node. In [33], a ZNN-based approach is applied to the range-free localization in WSN in an effective way.

It can be seen that ZNN can be applied to solve wireless localization problems efficiently. However, to the best of our knowledge, existing works for solving the time-varying WSN localization problem are considerably rare. In addition, as a special type of neurodynamics, zeroing neurodynamics (ZND) is generalized from ZNN and can guarantee that each element of the error function converges to zero [34], [35]. For this reason, a quite implementable and feasible ZND-based method for solving the range-based and time-varying WSN localization problem is provided.

III. WSN Localization Problem and ZND Solution

This section describes the AOA-based and TDOA-based WSN localization problems in the form of a dynamic matrix equation and provides the unified formulation of these problems. Afterwards, based on the unified formulation, the routine of the conventional ZND model for solving WSN localization problems is presented.

A. Localization Problem

In this paper, we consider the AOA algorithm in a 2-dimensional (2D) case and the TDOA algorithm in a 3-dimensional (3D) case. For simplicity, a small and localized topology in WSN is explored, where an unknown node estimates its own position with the assistance of several anchor nodes. Suppose the number of the anchor nodes is m ($m \geq 2$ for the AOA algorithm and $m \geq 5$ for the TDOA algorithm).

1) AOA Algorithm: For the AOA algorithm, the position of the unknown node is calculated by the measured arrival angle of the communication signal at the receiver, i.e., the anchor node. Consider a 2D mobile scenario, in which the position of the unknown node changes with time, and m anchor nodes are randomly placed and fixed. Then the localization problem of the moving unknown node in WSN is subsequently investigated. First, we define the coordinates of m anchor nodes and the unknown node as

$$M = \begin{bmatrix} x_1 & x_2 & \cdots & x_m \\ y_1 & y_2 & \cdots & y_m \end{bmatrix} \in \mathbb{R}^{2\times m}, \quad \mathbf{x}(t) = \begin{bmatrix} x(t) \\ y(t) \end{bmatrix} \in \mathbb{R}^2.$$

Second, according to the geometric meaning of AOA, the following equation is obtained:

$$\tan(\alpha_i(t)) = \frac{y(t) - y_i}{x(t) - x_i}, \tag{1}$$

where $i \in \{1, 2, \cdots, m\}$; $\alpha_i(t)$ denotes the arrival angle of the communication signal between unknown node and the ith anchor node. Then the above equation can be rewritten as

$$-\tan(\alpha_i(t))x(t) + y(t) = y_i - x_i \tan(\alpha_i(t)).$$

Finally, the AOA-based WSN localization problem on moving unknown node in 2D scenario is finally formulated as

$$\begin{bmatrix} -\tan(\alpha_1(t)) & 1 \\ -\tan(\alpha_2(t)) & 1 \\ \vdots & \vdots \\ -\tan(\alpha_m(t)) & 1 \end{bmatrix} \begin{bmatrix} x(t) \\ y(t) \end{bmatrix} = \begin{bmatrix} y_1 - x_1 \tan(\alpha_1(t)) \\ y_2 - x_2 \tan(\alpha_2(t)) \\ \vdots \\ y_m - x_m \tan(\alpha_m(t)) \end{bmatrix}. \tag{2}$$

2) TDOA Algorithm: The TDOA algorithm measures the time differences of the disparate arriving signals originated from the source to a number of spatially separated receivers, i.e., the anchor nodes, to estimate the position of the source, i.e., the unknown node. Different from subsection III-A1, a 3D mobile scenario is observed in this subsection. The coordinates of m anchor nodes and the unknown node are defined as

$$N = \begin{bmatrix} x_1 & x_2 & \cdots & x_m \\ y_1 & y_2 & \cdots & y_m \\ z_1 & z_2 & \cdots & z_m \end{bmatrix} \in \mathbb{R}^{3\times m}, \quad \mathbf{x}(t) = \begin{bmatrix} x(t) \\ y(t) \\ z(t) \end{bmatrix} \in \mathbb{R}^3.$$

According to the physical meaning of TDOA, we have the following equations [28]:

$$\begin{aligned} r_i(t) &= \upsilon T_i(t) \\ &= \sqrt{(x_i - x(t))^2 + (y_i - y(t))^2 + (z_i - z(t))^2}, \\ \Delta T_{i1}(t) &= T_i(t) - T_1(t), \\ r_{i1}(t) &= \upsilon \Delta T_{i1}(t) = r_i(t) - r_1(t), \end{aligned}$$

where $i \in \{1, 2, \cdots, m\}$; υ is the propagation speed of the communication signal between the unknown node and the

anchor node; $T_i(t)$ symbolizes the time of signal from the unknown node to the ith anchor node; $\Delta T_{i1}(t)$ represents the time difference of signal from the unknown node separately to the ith and first anchor nodes; $r_i(t)$ denotes the distance between the unknown node and the ith anchor node; $r_{i1}(t)$ denotes the distance difference from the unknown node to the ith and first anchor nodes. By the derivation in APPENDIX, the TDOA-based WSN localization problem on moving unknown node in 3D scenario can be formulated as

$$\begin{bmatrix} x_{21} & y_{21} & z_{21} & \upsilon\Delta T_{21}(t) \\ x_{31} & y_{31} & z_{31} & \upsilon\Delta T_{31}(t) \\ \vdots & \vdots & \vdots & \vdots \\ x_{m1} & y_{m1} & z_{m1} & \upsilon\Delta T_{m1}(t) \end{bmatrix} \begin{bmatrix} x(t) \\ y(t) \\ z(t) \\ r_1(t) \end{bmatrix} = \begin{bmatrix} (Q_2 - Q_1 - (\upsilon\Delta T_{21}(t))^2)/2 \\ (Q_3 - Q_1 - (\upsilon\Delta T_{31}(t))^2)/2 \\ \vdots \\ (Q_m - Q_1 - (\upsilon\Delta T_{m1}(t))^2)/2 \end{bmatrix}, \quad (3)$$

where $Q_i = {x_i}^2 + {y_i}^2 + {z_i}^2$.

3) Unified Formulation: From (2) and (3), it is easy to find that AOA-based and TDOA-based WSN localization problems can be finally unified into the following form:

$$\mathcal{P}(t)\mathbf{s}(t) = \mathbf{z}(t). \quad (4)$$

The above equation is a dynamic matrix equation, where $\mathcal{P}(t) \in \mathbb{R}^{p\times q}$ is a known coefficient matrix with $p, q \in \mathbb{Z}$ and involves the measured physical property of the communication signal, i.e., AOA or TDOA; $\mathbf{z}(t) \in \mathbb{R}^p$ is a known vector; $\mathbf{s}(t) \in \mathbb{R}^q$ is an unknown vector with $q = 2$ or $q = 4$, involving the coordinate of the unknown node to be solved. Consequently, the subsequent task of this work is to solve (4).

B. Conventional ZND Model

So far, many successes have been achieved for the design and application of ZND on dynamic problems. In the conventional ZND model [22], the WSN localization problem (4) is solved by the following three steps.

(1) Construct the error function $\mathbf{e}(t) = \mathcal{P}(t)\mathbf{s}(t) - \mathbf{z}(t) \in \mathbb{R}^p$.
(2) To guarantee that each element of $\mathbf{e}(t)$ converges to zero, the evolution equation is designed as $\dot{\mathbf{e}}(t) = -\gamma F(\mathbf{e}(t))$ where $\dot{\mathbf{e}}(t)$ denotes the time derivation of $\mathbf{e}(t)$; $\gamma > 0$ is a scaling factor; $F(\cdot) : \mathbb{R}^p \to \mathbb{R}^p$ stands for an array of AFs with each element being a linear function and denoted by $f(\cdot) : \mathbb{R} \to \mathbb{R}$.
(3) Substitute $\mathbf{e}(t)$ in step (1) into the evolution equation to obtain the conventional ZND solution for the WSN localization problem: $\dot{\mathcal{P}}(t)\mathbf{s}(t) + \mathcal{P}(t)\dot{\mathbf{s}}(t) - \dot{\mathbf{z}}(t) = -\gamma F(\mathcal{P}(t)\mathbf{s}(t) - \mathbf{z}(t))$.

Thus, the routine of the conventional ZND model for solving the WSN localization problem (4) is completed.

IV. Modified ZND Models

Based on ZND methodology, we further explore and propose two modified ZND models for solving the localization problem (4) in this section.

For simplicity, the error function in step (1) is adopted here: $\mathbf{e}(t) = \mathcal{P}(t)\mathbf{s}(t) - \mathbf{z}(t)$. The corresponding design formula is modified as

$$\dot{\mathbf{e}}(t) = -\varphi L(\mathbf{e}(t)), \quad (5)$$

where φ, a positive value, is used to scale the convergence rate of the ZND model. Different from the conventional ZND model, $L(\cdot) : \mathbb{R}^p \to \mathbb{R}(\cdot)^p$ stands for an array of AFs with each element being a monotonically-increasing odd function and denoted by $\mathcal{L}(\cdot) : \mathbb{R} \to \mathbb{R}$, such that each item of error function decreases to zero, and then the theoretical solution of (4) can be obtained. In view of practical WSN application scenarios, the localization problem (4) is often normal or overdetermined in mathematics. By employing the design formula (5), the ZND model for WSN localization problem (4) with normal situation (i.e., for $\mathcal{P}(t) \in \mathbb{R}^{p\times q}$ with $p = q$) is derived:

$$\dot{\mathbf{s}}(t) = \mathcal{P}^+(t)[\dot{\mathbf{z}}(t) - \dot{\mathcal{P}}(t)\mathbf{s}(t) - \varphi L(\mathcal{P}(t)\mathbf{s}(t) - \mathbf{z}(t))], \quad (6)$$

where $\mathcal{P}^+(t)$ denotes the pseudoinverse of matrix $\mathcal{P}(t)$. For the case of overdetermined localization problem with $p > q$, by taking the error function into (5), and multiplying both sides by $\mathcal{P}^{\mathrm{T}}(t)$ with superscript $^{\mathrm{T}}$ being the transpose operator, the ZND model has the form:

$$\mathcal{P}^{\mathrm{T}}(t)\mathcal{P}(t)\dot{\mathbf{s}}(t) = -\varphi\mathcal{P}^{\mathrm{T}}(t)L(\mathcal{P}(t)\mathbf{s}(t) - \mathbf{z}(t)) - \mathcal{P}^{\mathrm{T}}(t)\dot{\mathcal{P}}(t)\mathbf{s}(t) + \mathcal{P}^{\mathrm{T}}(t)\dot{\mathbf{z}}(t). \quad (7)$$

If $\mathcal{P}(t)$ is of full column rank, then $\mathcal{P}^{\mathrm{T}}(t)\mathcal{P}(t)$ is invertible and $\mathcal{P}^+(t) = (\mathcal{P}^{\mathrm{T}}(t)\mathcal{P}(t))^{-1}\mathcal{P}^{\mathrm{T}}(t)$ holds [36]. Thus, model (7) can be rewritten as

$$\dot{\mathbf{s}}(t) = \mathcal{P}^+(t)[\dot{\mathbf{z}}(t) - \dot{\mathcal{P}}(t)\mathbf{s}(t) - \varphi L(\mathcal{P}(t)\mathbf{s}(t) - \mathbf{z}(t))]. \quad (8)$$

Obviously, the formulations of model (6) and (8) are the same. Hence, based on model (8), the WSN localization problem (4) can be solved no matter with a normal or overdetermined situation.

Generally speaking, an AF acts as a projection operation from one set to another, and different choices for the AF lead to different convergence performances. Note that the conventional ZND model with the linear AF takes a long time to converge to the theoretical result. Therefore, in this section, based on model (8), two modified ZND models with different AFs are thus proposed to handle the WSN localization problem (4). The convergence performance is provided theoretically as well.

A. MZDL1 Model

As mentioned before, the ability of the ZND model (8) activated by the linear AF is limited. On the contrary, nonlinear AFs have attracted much attention in light of the superior convergence, and numerous related studies have been explored and investigated. Inspired by the work in [34], a specially-designed AF is firstly employed to activate the ZND model (8):

$$\mathcal{L}_1(x) = \kappa_1|x|^\tau \mathrm{sgn}(x) + \kappa_2|x|^\sigma \mathrm{sgn}(x), \quad (9)$$

where symbol $|\cdot|$ denotes the absolute value of a scalar; scaling factors $\kappa_1, \kappa_2 > 0$; design parameters $\tau \in (0, 1)$ and

$\sigma \in [1, \infty)$. In addition, the sign function $\mathrm{sgn}(x)$ [34] is defined as follows:

$$\mathrm{sgn}(x) = \begin{cases} 1, & x > 0, \\ 0, & x = 0, \\ -1, & x < 0. \end{cases} \tag{10}$$

By adding the above AF $\mathcal{L}_1(x)$ to model (8), a modified ZND model for solving the WSN localization problem (4) is given as

$$\dot{\mathbf{s}}(t) = \mathcal{P}^{+}(t)[\dot{\mathbf{z}}(t) - \dot{\mathcal{P}}(t)\mathbf{s}(t) - \varphi L_1(\mathcal{P}(t)\mathbf{s}(t) - \mathbf{z}(t))]. \tag{11}$$

For convenience, the modified model (11) is termed MZDL1 model in this paper. Then we have the following theorem on convergence of the MZDL1 model (11).

Theorem 1: Given a random and rough initial position $\mathbf{s}(0)$, the real-time position of the unknown node, which is estimated via the MZDL1 model (11), converges to the theoretical position $\mathbf{s}^*(t)$ in finite time

$$t_{\mathrm{L1}} \leq \frac{|\epsilon(0)|^{1-\tau}}{\varphi\kappa_1(1-\tau)},$$

where $\epsilon(0)$ denotes the element of position-vector $\mathbf{e}(0)$ with the largest absolute value.

Proof: From the aforementioned description, we know that, $\mathbf{s}^*(t)$ is the theoretical result of the WSN localization problem (4) based on AOA algorithm or TDOA algorithm. The state-position vector $\mathbf{s}(t)$ synthesized by the MZDL1 model (11) for solving these WSN localization problems, starting from a randomly-generated initial state $\mathbf{s}(0)$, converges to $\mathbf{s}^*(t)$ in finite time t_{L1}. According to the definition of the error function, when the error function converges to $\mathbf{0}$, $\mathbf{s}(t)$ approaches $\mathbf{s}^*(t)$. Therefore, position estimation $\mathbf{s}(t)$ can be investigated by discussing error function $\mathbf{e}(t)$. Next, rewrite the MZDL1 model (11) as $\dot{\mathbf{e}}(t) = -\varphi L_1(\mathbf{e}(t))$, of which the ith subsystem can be defined as

$$\dot{e}_i(t) = -\varphi\mathcal{L}_1(e_i(t)).$$

Then, define $\epsilon(t)$ be the element of the vector $\mathbf{e}(t)$ with the largest absolute value, i.e., $|\epsilon(t)| \geq |e_i(t)|$ for all i $(i = 1, 2, \ldots, p)$ at time instant t. Depending on the sign of $\epsilon(0)$, the analyses can be divided into the following three situations.

- For the first situation of $\epsilon(0) > 0$, according to $|\epsilon(t)| \geq |e_i(t)|$, we have $\epsilon(t) \geq |e_i(t)|$. This means that $e_i(t)$ converges to zero when $\epsilon(t)$ reaches zero. Let t_ϵ denote the convergence time of $\epsilon(t)$. That is, the MZDL1 model (11) converges to the theoretical result $\mathbf{s}^*(t)$ at time instant t_ϵ when solving WSN localization problem (4). Additionally, based on the definition of $\mathcal{L}_1(x)$, we have the following equation for calculating t_ϵ:

  $$\dot{\epsilon}(t) = -\varphi(\kappa_1\epsilon^{\tau}(t) + \kappa_2\epsilon^{\sigma}(t)).$$

  Since $\kappa_2\epsilon^{\sigma}(t) > 0$, we have

  $$\dot{\epsilon}(t) < -\varphi\kappa_1\epsilon^{\tau}(t).$$

  The above equation can be redefined as

  $$\mathrm{dt} < -\frac{1}{\varphi\kappa_1}\epsilon^{-\tau}(t)\mathrm{d}\epsilon(t).$$

  Integrating on both sides of the above equation generates

  $$\int_0^{t_\epsilon} \mathrm{dt} < -\frac{1}{\varphi\kappa_1}\int_{\epsilon(0)}^{0} \epsilon^{-\tau}(t)\mathrm{d}\epsilon(t).$$

  Solving the above equation obtains

  $$t_\epsilon < \frac{(\epsilon(0))^{1-\tau}}{\varphi\kappa_1(1-\tau)} = \frac{|\epsilon(0)|^{1-\tau}}{\varphi\kappa_1(1-\tau)}.$$

- For the second situation $\epsilon(0) < 0$, through similar procedure, convergence time t_ϵ is thus derived:

  $$t_\epsilon < \frac{(-\epsilon(0))^{1-\tau}}{\varphi\kappa_1(1-\tau)} = \frac{|\epsilon(0)|^{1-\tau}}{\varphi\kappa_1(1-\tau)}.$$

- For the third situation $\epsilon(0) = 0$, we finally have

  $$t_\epsilon = 0 = \frac{|\epsilon(0)|^{1-\tau}}{\varphi\kappa_1(1-\tau)}.$$

■

From the previous analyses of the three situations, it is concluded that, MZDL1 model (11) converges to the theoretical result $\mathbf{s}^*(t)$ in finite time t_{L1} when solving WSN localization problem (4). That is, synthesized by the MZDL1 model (11), the real-time position of the unknown node converges to $\mathbf{s}^*(t)$ in finite time t_{L1}, which is calculated as follows:

$$t_{\mathrm{L1}} = t_\epsilon \leq \frac{|\epsilon(0)|^{1-\tau}}{\varphi\kappa_1(1-\tau)}.$$

B. MZDL2 Model

To further explore the applicability of the ZND methodology in WSN, another special nonlinear AF is constructed to accelerate convergence time of model (8) for solving WSN localization problem (4), which is shown as

$$\mathcal{L}_2(x) = \varrho(\exp(\theta x) - \exp(-\theta x)), \tag{12}$$

where the design parameters $\theta \geq 1$, and the scaling factor $\varrho > 0$. Based on $\mathcal{L}_2(x)$, another modified ZND model (called MZDL2 model) is presented as

$$\dot{\mathbf{s}}(t) = \mathcal{P}^{+}(t)[\dot{\mathbf{z}}(t) - \dot{\mathcal{P}}(t)\mathbf{s}(t) - \varphi L_2(\mathcal{P}(t)\mathbf{s}(t) - \mathbf{z}(t))]. \tag{13}$$

For the MZDL2 model (13), we have the following theorem on its convergence.

Theorem 2: Given a random and rough initial position $\mathbf{s}(0)$, the real-time position of the unknown node, which is estimated via the MZDL2 model (13), converges to the theoretical position $\mathbf{s}^*(t)$ globally.

Proof: From the aforementioned description, we know that, $\mathbf{s}^*(t)$ is the theoretical result of the WSN localization problem (4) based on AOA algorithm or TDOA algorithm. If AF $\mathcal{L}_2(x)$ is used, the state-position vector $\mathbf{s}(t)$ synthesized by the MZDL2 model (13), beginning with any initial state $\mathbf{s}(0)$, can converge to $\mathbf{s}^*(t)$ globally. Similar to the proof in Theorem 1, position estimation $\mathbf{s}(t)$ is analyzed by considering the error function $\mathbf{e}(t)$. Inspired by the proof process of convergence analysis in [37], [38], we define a Lyapunov function candidate $V(t) = \|\mathbf{e}(t)\|_2^2/2$ for the MZDL2 model (13). Then the time derivative of $V(t)$ is $\dot{V}(t) = \mathbf{e}^{\mathrm{T}}(t)\dot{\mathbf{e}}(t)$. Let $e_i(t)$

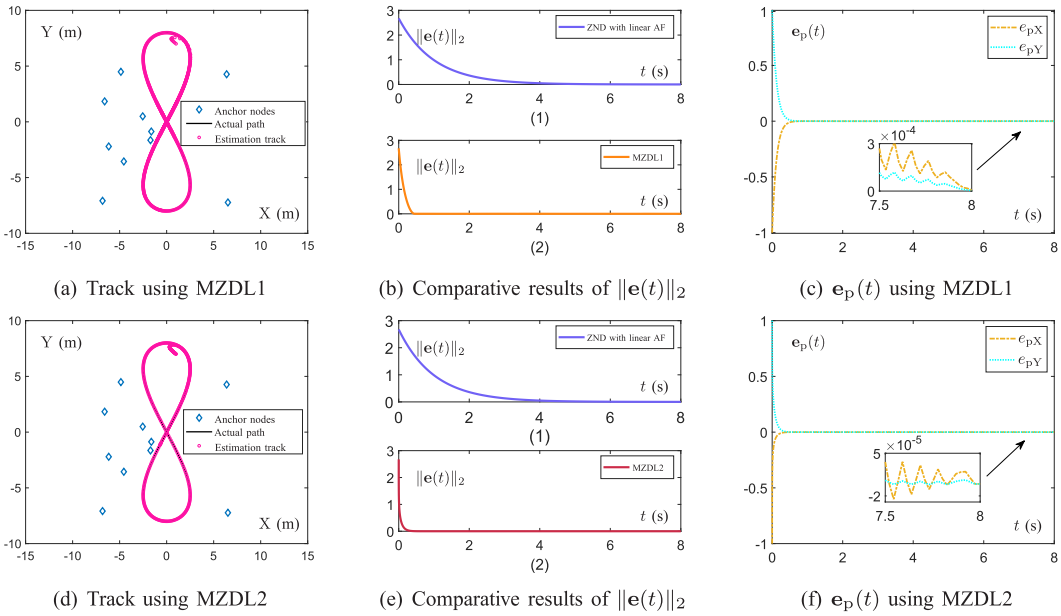

(a) Track using MZDL1 (b) Comparative results of $\|\mathbf{e}(t)\|_2$ (c) $\mathbf{e}_{\mathrm{p}}(t)$ using MZDL1

(d) Track using MZDL2 (e) Comparative results of $\|\mathbf{e}(t)\|_2$ (f) $\mathbf{e}_{\mathrm{p}}(t)$ using MZDL2

Fig. 1. Validation results of AOA-based WSN localization synthesized by MZDL1 model (11) and MZDL2 model (13) with the initial state $\mathrm{s}(0)$ randomly initialized, where $\varphi = 1$; $\kappa_1 = 1$; $\tau = 0.2$; $\kappa_2 = 6$; $\sigma = 5$; $\varrho = 2$; $\theta = 3$.

$(i = 1, 2, \ldots, p)$ denote the ith subsystem of $\mathbf{e}(t)$ and take (5) into account, then $V(t)$ and $\dot{V}(t)$ can be rewritten as

$$V(t) = \sum_{i=1}^{p} e_i^2(t)/2 \geq 0,$$

and

$$\dot{V}(t) = \sum_{i=1}^{p} e_i(t)\dot{e}_i(t) = -\varphi \sum_{i=1}^{p} e_i(t)\mathcal{L}_2(e_i(t)).$$

By Taylor expansion, $\mathcal{L}_2(e_i(t))$ is formulated as

$$\begin{aligned}\mathcal{L}_2(e_i(t)) &= \varrho[\exp(\theta e_i(t)) - \exp(-\theta e_i(t))] \\ &= 2\varrho\left[\theta e_i(t) + \frac{\theta^3 e_i^3(t)}{3!} + \frac{\theta^5 e_i^5(t)}{5!} + \cdots\right] \\ &= 2\varrho \sum_{r=1}^{+\infty} \frac{\theta^{2r-1}(e_i(t))^{2r-1}}{(2r-1)!}.\end{aligned}$$

Finally, $\dot{V}(t)$ is shown as

$$\begin{aligned}\dot{V}(t) &= -\delta \sum_{i=1}^{p} e_i(t) \sum_{r=1}^{+\infty} \frac{\theta^{2r-1}(e_i(t))^{2r-1}}{(2r-1)!} \\ &= -\delta \sum_{i=1}^{p} \sum_{r=1}^{+\infty} \frac{\theta^{2r-1}(e_i(t))^{2r}}{(2r-1)!} \leq 0,\end{aligned}$$

where $\delta = 2\varphi\varrho > 0$. So, if AF $\mathcal{L}_2(x)$ is used, we have $V(t) \geq 0$ and $\dot{V}(t) \leq 0$. In consideration of the Lyapunov theory, it is thus summarized that, the error function $\mathbf{e}(t)$ of the MZDL2 model (13) can converge to zero with time. That is, the MZDL2 model (13) converges to the theoretical result $\mathbf{s}^*(t)$ with time when solving WSN localization problem (4). In other words, synthesized by the MZDL2 model (13), the real-time position of the unknown node converges to the theoretical position globally. ■

V. Simulation Results and Validation

In this section, first of all, the AOA-based and TDOA-based localization simulations are performed to demonstrate the effectiveness of the MZDL1 model (11) and the MZDL2 model (13) for solving the WSN localization problem (4). Then, these two modified ZND models are applied to underwater sensor node localization on a testbed to illustrate the potential applicability of these models in UAN. Finally, a comparison of the MZDL2 model (13) with the multidimensional Kalman Filter algorithm is performed.

A. AOA-Based WSN Localization

In this section, we perform computer simulations on AOA-based WSN localization by separately utilizing the MZDL1 model (11) and the MZDL2 model (13). For simplicity, a 2D topology with a range of 20 m × 20 m is explored, where the unknown node moves along a lemniscate path, and 10 anchor nodes are randomly deployed and fixed. There are six subgraphs in Fig. 1, with subgraphs (a), (b-2), and (c) generated from the MZDL1 model (11) and subgraphs (d), (e-2), and (f) generated from the MZDL2 model (13). Meanwhile, the comparative results synthesized by the conventional ZND model with the linear AF are given in subgraphs (b-1) and (e-1).

To be specific, in Fig. 1(a) and (d), the anchor nodes are denoted by diamonds, the actual lemniscate path of the unknown node moving is described by the black solid line, and the estimate track of unknown node moving is depicted by the pink circle marker. As it is clear, the two trajectories are almost coincident. The residual errors $\|\mathbf{e}(t)\|_2$ synthesized by modified models we proposed compared with the conventional ZND model with the linear AF are presented in Fig. 1(b) and (e). It is worth noting that residual errors $\|\mathbf{e}(t)\|_2$ using the modified ZND model (11) and model (13)

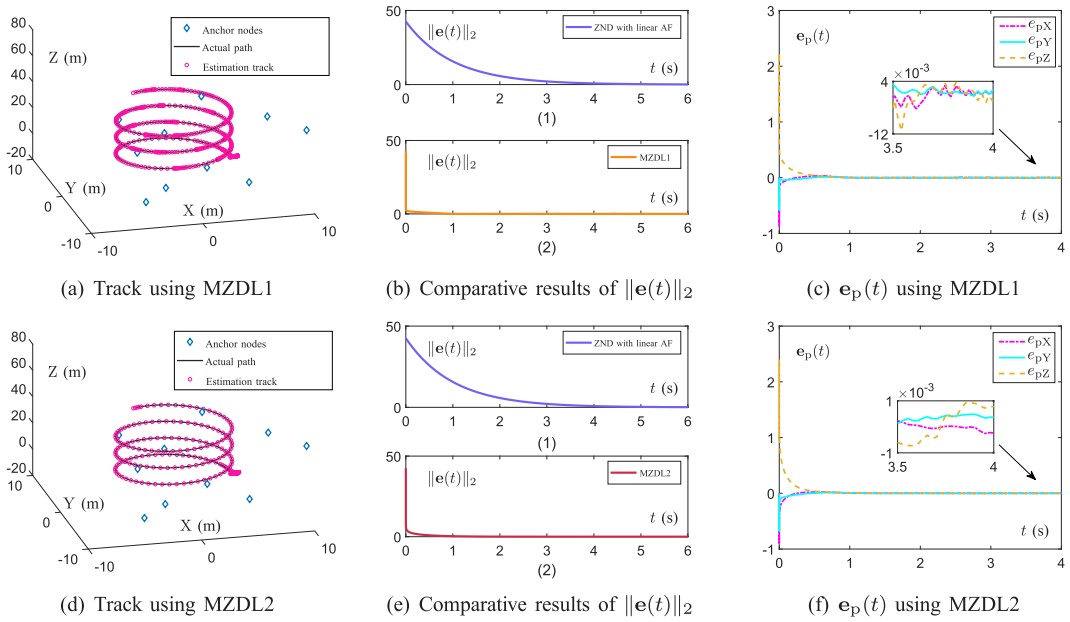

(a) Track using MZDL1 (b) Comparative results of $\|\mathbf{e}(t)\|_2$ (c) $\mathbf{e}_{\mathrm{p}}(t)$ using MZDL1

(d) Track using MZDL2 (e) Comparative results of $\|\mathbf{e}(t)\|_2$ (f) $\mathbf{e}_{\mathrm{p}}(t)$ using MZDL2

Fig. 2. Validation results of TDOA-based WSN localization synthesized by MZDL1 model (11) and MZDL2 model (13) with the initial position of unknown node randomly initialized, where $\varphi = 1$; $\kappa_1 = 1$; $\tau = 0.2$; $\kappa_2 = 6$; $\sigma = 10$; $\varrho = 0.5$; $\theta = 2$.

converge much faster than that using the conventional ZND model with the linear AF. Figure 1(c) and (f) describe the position estimation errors $\mathbf{e}_{\mathrm{p}}(t) = \mathbf{s}(t) - \mathbf{s}^*(t) = [e_{\mathrm{pX}}, e_{\mathrm{pY}}]^{\mathrm{T}}$, from which we can see that both e_{pX} and e_{pY} converge to 0 m quickly. For most WSN applications, the localization accuracy of these two models is already sufficient.

Overall, the proposed ZND models (11) and (13) are successfully applied to the moving position estimation in AOA-based WSN localization, with satisfactory verification results.

B. TDOA-Based WSN Localization

In this section, computer simulations on TDOA-based WSN localization are carried out, and the validation results obtained by the MZDL1 model (11) are depicted in Fig. 2(a), (b-2), and (c), and the validation results corresponding to the MZDL2 model (13) are described in Fig. 2(d), (e-2), (f). Meanwhile, the comparative results synthesized by the conventional ZND model with the linear AF are given in subgraphs (b-1) and (e-1).

Specifically, as visualized in Fig. 2(a) and (d), 10 anchor nodes denoted by diamonds are randomly deployed and fixed in a 3D topology with a range of 20 m × 20 m × 100 m, and the unknown node moves along a spiral path denoted by the black solid line. It can be found that the pink circles-marked estimation tracks generated by MZDL1 model (11) and the MZDL2 model (13) are almost coincident with the actual paths of the unknown node. As presented in Fig. 2(b) and (e), residual errors $\|\mathbf{e}(t)\|_2$ using the modified ZND model (11) and model (13) converge much faster than that using the conventional ZND model with the linear AF. As for Fig. 2(c) and (f), the validation results of these two models with the position estimation error $\mathbf{e}_{\mathrm{p}}(t) = [e_{\mathrm{pX}}, e_{\mathrm{pY}}, e_{\mathrm{pZ}}]^{\mathrm{T}}$ being the order of 10^{-3} m manifest the abilities of the proposed models to deal with the TDOA-based WSN localization problem.

As a conclusion, the simulations conducted on the real-time position estimation in TDOA-based WSN localization problem verify the dynamic robustness and accuracy of the proposed MZDL1 model (11) and MZDL2 model (13).

C. Application to UAN Testbed

Underwater acoustic network, also termed underwater WSN, is a special and challenging WSN where the sensor nodes are deployed underwater and communicate through acoustic signals. Due to the advantage of acoustic waves propagating over long distances underwater, UAN finds wide applications in marine scientific exploration, marine engineering construction, and seabed mineral resources survey [39], [40]. Most of them depend on the position information of sensor nodes. Therefore, localization is a key and fundamental technology in UAN. In the last few years, we have managed to build a UAN testbed assembled Micro-ANP protocol stack [41], [42] and conduct many trials on Qinghai Lake to monitor the water quality by means of underwater acoustic communication. In this section, some geographic coordinates (i.e., spherical coordinates of ground point positions expressed in latitude and longitude) marking the positions of underwater sensor nodes of the testbed are utilized to simulate the AOA-based localization synthesized by the MZDL1 model (11) and the MZDL2 model (13). The validation results prove the potential practicability of these two models.

As shown in Fig. 3, the testbed is mainly composed of one industrial router, five sets of nodes, and one remote server. Each set of node consists primarily of a C15 CTD sensor, AquaSeNT OFDM acoustic modem, and Raspberry PI3 control board. Moreover, some physical parameters and technical specifications of the UAN testbed are displayed in TABLE II. The "Testbed Deployment" in Fig. 3 contains some working shootings which show how we build the testbed.

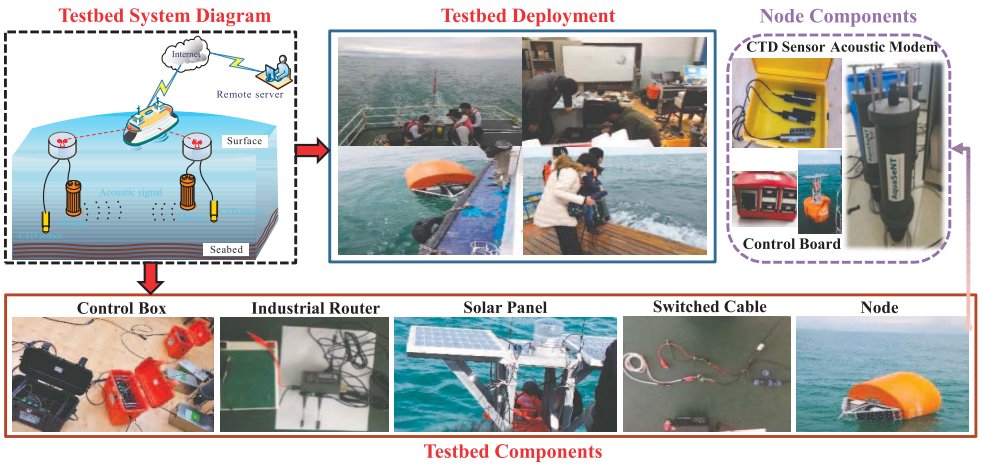

Fig. 3. The system diagram of UAN testbed built on Qinghai Lake.

TABLE II
TECHNICAL SPECIFICATIONS OF THE UAN TESTBED

Instrument	Parameter	Value
Acoustic modem	Depth (m)	3
	Range (km)	5
	Frequency (kHz)	21∼27
	Supply (VDC)	12∼16
CTD sensor	Sampling frequency (kHz)	1
	Supply (VDC)	12∼16
Control board	Model	Raspberry Pi 3b
	Supply (VDC)	5

TABLE III
THE GEOGRAPHIC COORDINATES OF FIVE SENSOR NODES

Node	Latitude(°N)	Longitude(°E)	Equipped with GPS
A_1	36.712688	100.504772	✓
A_2	36.675523	100.521251	✓
A_3	36.733602	100.551464	✓
A_4	36.692043	100.567256	✓
U_1	36.706770	100.544254	✗

Incidentally, the depth difference among nodes is negligible in this experiment, the speed of water flow is also not taken into account so that the nodes are deemed to be static.

Afterwards, the AOA-based UAN localization experiments are conducted, and the verification results are illustrated in Fig. 4. Figure 4(a) and (c) present the unknown node U_1 marked by a cyan star and the evolutionary track of $\mathbf{s}(t)$ marked by red circles, while Fig. 4(b) and (d) show the convergence of position estimation error $\mathbf{e}_{\mathrm{p}}(t)$. Nodes from A_1 to A_4 are anchor nodes equipped with GPS modules, and their geographic coordinates are listed in TABLE III. Node U_1 is the unknown node with the geographic coordinate to be solved. The actual position of the unknown node can be properly estimated by the modified ZND models (i.e., (11) and (13)). It can be stated that the MZDL1 model (11) and the MZDL2 model (13) are also valid for addressing the static problem of AOA-based UAN localization on the testbed.

On account of high difficulty and cost, most research is mainly based on theoretical analysis and network simulators. The validation results about the UAN testbed in this section illustrate the potential applicabilities of the proposed ZND models for solving UAN localization problem and, more importantly, provide a basis for further implementation of the modified ZND models to UANs.

D. Comparison With the Kalman Filter

In this section, we perform a comparison of vehicle location between the MZDL2 model (13) with the multidimensional Kalman Filter algorithm in the following example. Parameters and definitions employed in the multidimensional Kalman Filter algorithm are listed in TABLE I in Introduction. The comparative results are displayed in Fig. 5.

In this example, the vehicle equipped with a sensor can obtain the coordinates information by communicating with the surrounding sensor nodes. Besides, we assume that the vehicle moves with a constant acceleration. Then, Kalman Filter equations in matrix are derived as

$$\begin{aligned}
\hat{\boldsymbol{x}}_{\boldsymbol{k+1,k}} &= F\hat{\boldsymbol{x}}_{\boldsymbol{k,k}} + B\boldsymbol{u}_{\boldsymbol{k}} \\
P_{k+1,k} &= FP_{k,k}F^{\mathrm{T}} + Q \\
G_{k+1} &= P_{k+1,k}H^{\mathrm{T}}(HP_{k+1,k}H^{\mathrm{T}} + R)^{-1} \\
\hat{\boldsymbol{x}}_{\boldsymbol{k+1,k+1}} &= \hat{\boldsymbol{x}}_{\boldsymbol{k+1,k}} + G_{k+1}(\boldsymbol{z}_{\boldsymbol{k+1}} - H\hat{\boldsymbol{x}}_{\boldsymbol{k+1,k}}) \\
P_{k+1,k+1} &= (I - G_{k+1})P_{k+1,k},
\end{aligned}$$

where $\boldsymbol{u}_{\boldsymbol{k}}$, $\hat{\boldsymbol{x}}_{\boldsymbol{k,k}}$, F and B are respectively defined by

$$\boldsymbol{u}_{\boldsymbol{k}} = \vec{a}, \quad \hat{\boldsymbol{x}}_{\boldsymbol{k,k}} = \begin{bmatrix} x_k \\ v_k^x \\ y_k \\ v_k^y \end{bmatrix},$$

$$F = \begin{bmatrix} 1 & \Delta T & 0 & 0 \\ 0 & 1 & 0 & 0 \\ 0 & 0 & 1 & \Delta T \\ 0 & 0 & 0 & 1 \end{bmatrix}, \quad B = \begin{bmatrix} \frac{\Delta T^2}{2} \\ 0 \\ \frac{\Delta T^2}{2} \\ 0 \end{bmatrix}.$$

As shown in Fig. 5(a) and (c), the true value of the vehicle position is denoted by the green line, and the estimate value is painted by the pink line with circles or triangles. It can be found that the pink triangles-marked estimate value generated

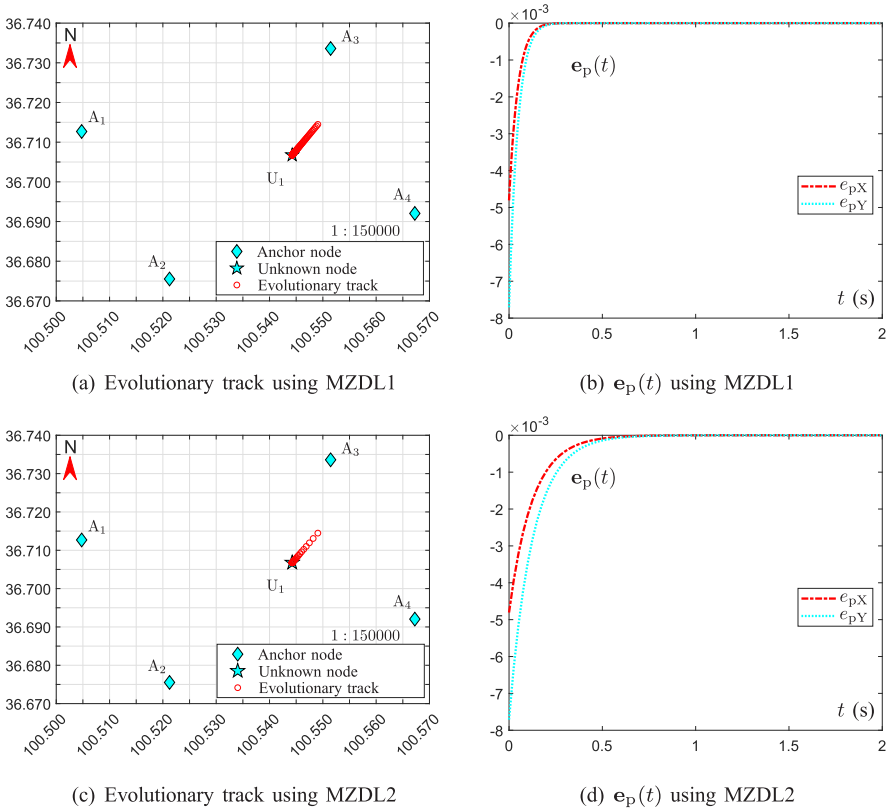

(a) Evolutionary track using MZDL1

(b) $\mathbf{e}_{\mathrm{p}}(t)$ using MZDL1

(c) Evolutionary track using MZDL2

(d) $\mathbf{e}_{\mathrm{p}}(t)$ using MZDL2

Fig. 4. Validation results of AOA-based UAN localization synthesized by MZDL1 model (11) and MZDL2 model (13) with the initial state randomly set, where $\varphi = 4$; $\kappa_1 = 2$; $\tau = 0.9$; $\kappa_2 = 2$; $\sigma = 1$; $\varrho = 0.5$; $\theta = 2$.

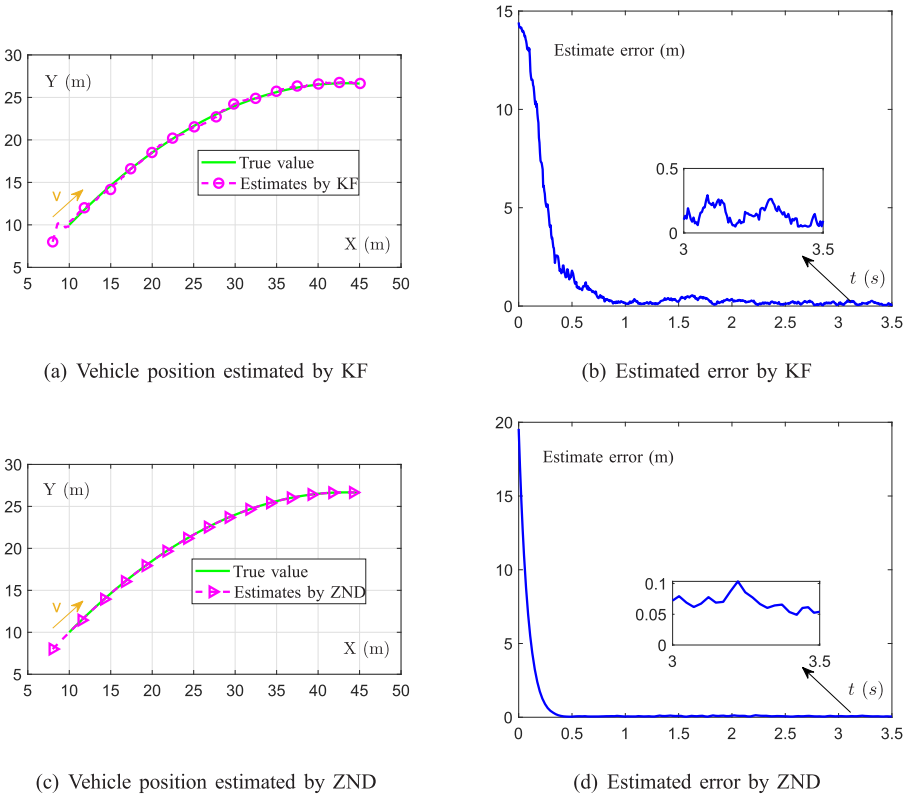

(a) Vehicle position estimated by KF

(b) Estimated error by KF

(c) Vehicle position estimated by ZND

(d) Estimated error by ZND

Fig. 5. Comparative results synthesized by the KF algorithm and the modified ZND model (using MZDL2) in the example of vehicle location.

by the modified ZND model (using the MZDL2 model (13)) is more coincident with the true value than that by the KF algorithm. As presented in Fig. 5(b) and (d), the estimated error by the modified ZND model (13) is lower than that by the KF algorithm. In addition, it converges faster and more smoothly than the latter. Thus, it can be concluded that the

modified ZND model (13) has the advantages in stability, locating accuracy, as well as convergent speed compared with the KF algorithm.

VI. Conclusions

In this paper, the applicability of the ZND methodology has been explored and extended to the WSN and the UAN. Two modified ZND models (i.e., the MZDL1 model and the MZDL2 model) have been proposed to deal with the WSN localization problem. Besides, the convergence properties of these two models have been rigorously analyzed in detail. In simulations, the two proposed models have been successfully employed in range-based WSN localization from AOA and TDOA measurements to demonstrate their effectiveness in the terms of high accuracy and dynamic robustness to the environment. Furthermore, the application to underwater sensor node localization of the UAN testbed has illustrated the feasibilities of the modified ZND models for solving the UAN localization problem, and more importantly, it has provided a basis for further implementation of the modified ZND models to UANs.

Appendix

It is deduced from the definition of $r_i(t)$ that

$$r_i^2(t) = {x_i}^2 + {y_i}^2 + {z_i}^2 - 2x_i x(t) - 2y_i y(t) - 2z_i z(t) + x^2(t) + y^2(t) + z^2(t),$$

and when $i = 1$,

$$r_1^2(t) = {x_1}^2 + {y_1}^2 + {z_1}^2 - 2x_1 x(t) - 2y_1 y(t) - 2z_1 z(t) + x^2(t) + y^2(t) + z^2(t).$$

Let $Q_i = {x_i}^2 + {y_i}^2 + {z_i}^2$, the above two equations can be rewritten as:

$$r_i^2(t) = Q_i - 2x_i x(t) - 2y_i y(t) - 2z_i z(t) + x^2(t) + y^2(t) + z^2(t), \tag{14}$$

$$r_1^2(t) = Q_1 - 2x_1 x(t) - 2y_1 y(t) - 2z_1 z(t) + x^2(t) + y^2(t) + z^2(t). \tag{15}$$

Considering the definition $r_{i1}(t) = r_i(t) - r_1(t)$, subtracting (15) from (14) results in

$$\begin{aligned} left &= r_i^2(t) - r_1^2(t) \\ &= (r_i(t) - r_1(t))^2 + 2r_i(t)r_1(t) - 2r_1^2(t) \\ &= r_{i1}^2(t) + 2r_1(t)(r_i(t) - r_1(t)) \\ &= r_{i1}^2(t) + 2r_1(t)r_{i1}(t), \end{aligned}$$

and

$$right = Q_i - Q_1 - 2x_{i1}x(t) - 2y_{i1}y(t) - 2z_{i1}z(t),$$

where $x_{i1} = x_i - x_1$, $y_{i1} = y_i - y_1$, and $z_{i1} = z_i - z_1$. Then, combing *left* and *right* leads to

$$x_{i1}x(t) + y_{i1}y(t) + z_{i1}z(t) + r_1(t)r_{i1}(t) = \frac{1}{2}(Q_i - Q_1 - r_{i1}^2(t)).$$

Considering the definition $r_{i1}(t) = \upsilon \Delta T_{i1}(t)$, as a result, it yields the following equation:

$$\begin{bmatrix} x_{21} & y_{21} & z_{21} & \upsilon\Delta T_{21}(t) \\ x_{31} & y_{31} & z_{31} & \upsilon\Delta T_{31}(t) \\ \vdots & \vdots & \vdots & \vdots \\ x_{m1} & y_{m1} & z_{m1} & \upsilon\Delta T_{m1}(t) \end{bmatrix} \begin{bmatrix} x(t) \\ y(t) \\ z(t) \\ r_1(t) \end{bmatrix} = \begin{bmatrix} (Q_2 - Q_1 - (\upsilon\Delta T_{21}(t))^2)/2 \\ (Q_3 - Q_1 - (\upsilon\Delta T_{31}(t))^2)/2 \\ \vdots \\ (Q_m - Q_1 - (\upsilon\Delta T_{m1}(t))^2)/2 \end{bmatrix}.$$

References

[1] G. Jones, "Echolocation," *Current Biol.*, vol. 15, no. 13, pp. 484–488, 2005.

[2] E. S. Bridge *et al.*, "Technology on the move: Recent and forthcoming innovations for tracking migratory birds," *BioScience*, vol. 61, no. 9, pp. 689–698, Sep. 2011.

[3] A. A. Kannan, B. Fidan, and G. Mao, "Analysis of flip ambiguities for robust sensor network localization," *IEEE Trans. Veh. Technol.*, vol. 59, no. 4, pp. 2057–2070, May 2010.

[4] W. Li, Y. Hu, X. Fu, S. Lu, and D. Chen, "Cooperative positioning and tracking in disruption tolerant networks," *IEEE Trans. Parallel Distrib. Syst.*, vol. 26, no. 2, pp. 382–391, Feb. 2015.

[5] M. Farooq-I-Azam, Q. Ni, and E. A. Ansari, "Intelligent energy efficient localization using variable range beacons in industrial wireless sensor networks," *IEEE Trans. Ind. Informat.*, vol. 12, no. 6, pp. 2206–2216, Dec. 2016.

[6] F. Yin, C. Fritsche, D. Jin, F. Gustafsson, and A. M. Zoubir, "Cooperative localization in WSNs using Gaussian mixture modeling: Distributed ECM algorithms," *IEEE Trans. Signal Process.*, vol. 63, no. 6, pp. 1448–1463, Mar. 2015.

[7] K. Derr and M. Manic, "Wireless sensor networks—Node localization for various industry problems," *IEEE Trans. Ind. Informat.*, vol. 11, no. 3, pp. 752–762, Jun. 2015.

[8] P. R. Gautam, S. Kumar, A. Verma, T. Rashid, and A. Kumar, "Energy-efficient localization of sensor nodes in WSNs using beacons from rotating directional antenna," *IEEE Trans. Ind. Informat.*, vol. 15, no. 11, pp. 5827–5836, Nov. 2019.

[9] J. Rezazadeh, M. Moradi, A. S. Ismail, and E. Dutkiewicz, "Superior path planning mechanism for mobile beacon-assisted localization in wireless sensor networks," *IEEE Sensors J.*, vol. 14, no. 9, pp. 3052–3064, Sep. 2014.

[10] K. Sabale, S. Sapre, and S. Mini, "Obstacle handling mechanism for mobile anchor assisted localization in wireless sensor networks," *IEEE Sensors J.*, vol. 21, no. 19, pp. 21999–22010, Oct. 2021.

[11] S. Salari, S. ShahbazPanahi, and K. Ozdemir, "Mobility-aided wireless sensor network localization via semidefinite programming," *IEEE Trans. Wireless Commun.*, vol. 12, no. 12, pp. 5966–5978, Dec. 2013.

[12] K. Zheng *et al.*, "Energy-efficient localization and tracking of mobile devices in wireless sensor networks," *IEEE Trans. Veh. Technol.*, vol. 66, no. 3, pp. 2714–2726, Mar. 2017.

[13] T. He, C. Huang, B. M. Blum, J. A. Stankovic, and T. Abdelzaher, "Range-free localization schemes for large scale sensor networks," in *Proc. 9th Annu. Int. Conf. Mobile Comput. Netw. (MobiCom)*, San Diego, CA, USA, 2003, pp. 81–95.

[14] G. Han, J. Jiang, C. Zhang, T. Q. Duong, M. Guizani, and G. K. Karagiannidis, "A survey on mobile anchor node assisted localization in wireless sensor networks," *IEEE Commun. Surveys Tuts.*, vol. 18, no. 3, pp. 2220–2243, 3rd Quart., 2016.

[15] A. Mukherjee, P. Goswami, and L. Yang, "DAI based wireless sensor network for multimedia applications," *Multimedia Tools Appl.*, vol. 80, no. 11, pp. 16619–16633, May 2021.

[16] S. Rajasoundaran *et al.*, "Secure routing with multi-watchdog construction using deep particle convolutional model for IoT based 5G wireless sensor networks," *Comput. Commun.*, vol. 187, pp. 71–82, Apr. 2022.

[17] P. Goswami, Z. Yan, A. Mukherjee, L. Yang, S. Routray, and G. Palai, "An energy efficient clustering using firefly and HML for optical wireless sensor network," *Optik*, vol. 182, pp. 181–185, Apr. 2019.

[18] L. Wei, L. Jin, C. Yang, K. Chen, and W. Li, "New noise-tolerant neural algorithms for future dynamic nonlinear optimization with estimation on Hessian matrix inversion," *IEEE Trans. Syst., Man, Cybern., Syst.*, vol. 51, no. 4, pp. 2611–2623, Apr. 2021.
[19] M. Liu, L. Chen, X. Du, L. Jin, and M. Shang, "Activated gradients for deep neural networks," *IEEE Trans. Neural Netw. Learn. Syst.*, early access, Sep. 1, 2021, doi: 10.1109/TNNLS.2021.3106044.
[20] L. Wei, L. Jin, and X. Luo, "Noise-suppressing neural dynamics for time-dependent constrained nonlinear optimization with applications," *IEEE Trans. Syst., Man, Cybern. Syst.*, early access, Jan. 6, 2022, doi: 10.1109/TSMC.2021.3138550.
[21] L. Jin, L. Wei, and S. Li, "Gradient-based differential neural-solution to time-dependent nonlinear optimization," *IEEE Trans. Autom. Control*, early access, Jan. 20, 2022, doi: 10.1109/TAC.2022.3144135.
[22] Y. Zhang, D. Jiang, and J. Wang, "A recurrent neural network for solving Sylvester equation with time-varying coefficients," *IEEE Trans. Neural Netw.*, vol. 13, no. 5, pp. 1053–1063, Sep. 2002.
[23] L. Xiao, H. Tan, L. Jia, J. Dai, and Y. Zhang, "New error function designs for finite-time ZNN models with application to dynamic matrix inversion," *Neurocomputing*, vol. 402, pp. 395–408, Aug. 2020.
[24] Z. Xie, L. Jin, X. Du, X. Xiao, H. Li, and S. Li, "On generalized RMP scheme for redundant robot manipulators aided with dynamic neural networks and nonconvex bound constraints," *IEEE Trans. Ind. Informat.*, vol. 15, no. 9, pp. 5172–5181, Sep. 2019.
[25] M. Yang, Y. Zhang, and H. Hu, "Discrete ZNN models of adams-bashforth (AB) type solving various future problems with motion control of mobile manipulator," *Neurocomputing*, vol. 384, pp. 84–93, Apr. 2020.
[26] D. Chen, X. Cao, and S. Li, "A multi-constrained zeroing neural network for time-dependent nonlinear optimization with application to mobile robot tracking control," *Neurocomputing*, vol. 460, pp. 331–344, Oct. 2021.
[27] A. T. Khan, X. Cao, Z. Li, and S. Li, "Enhanced beetle antennae search with zeroing neural network for online solution of constrained optimization," *Neurocomputing*, vol. 447, pp. 294–306, Aug. 2021.
[28] L. Jin, J. Yan, X. Du, X. Xiao, and D. Fu, "RNN for solving time-variant generalized Sylvester equation with applications to robots and acoustic source localization," *IEEE Trans. Ind. Informat.*, vol. 16, no. 10, pp. 6359–6369, Oct. 2020.
[29] Y. Qi, L. Jin, H. Li, Y. Li, and M. Liu, "Discrete computational neural dynamics models for solving time-dependent Sylvester equation with applications to robotics and MIMO systems," *IEEE Trans. Ind. Informat.*, vol. 16, no. 10, pp. 6231–6241, Oct. 2020.
[30] L. Jin and Y. Zhang, "Discrete-time Zhang neural network for online time-varying nonlinear optimization with application to manipulator motion generation," *IEEE Trans. Neural Netw. Learn. Syst.*, vol. 26, no. 7, pp. 1525–1531, Jul. 2015.
[31] L. Jin and Y. Zhang, "Continuous and discrete Zhang dynamics for real-time varying nonlinear optimization," *Numer. Algorithms*, vol. 73, pp. 115–140, Sep. 2016.
[32] L. Jin, Z. Xie, M. Liu, K. Chen, C. Li, and C. Yang, "Novel joint-drift-free scheme at acceleration level for robotic redundancy resolution with tracking error theoretically eliminated," *IEEE/ASME Trans. Mechatronics*, vol. 26, no. 1, pp. 90–101, Feb. 2021.
[33] S. Li and F. Qin, "A dynamic neural network approach for solving nonlinear inequalities defined on a graph and its application to distributed, routing-free, range-free localization of WSNs," *Neurocomputing*, vol. 117, pp. 72–80, Oct. 2013.
[34] L. Jin, S. Li, H. Wang, and Z. Zhang, "Nonconvex projection activated zeroing neurodynamic models for time-varying matrix pseudoinversion with accelerated finite-time convergence," *Appl. Soft Comput.*, vol. 62, pp. 840–850, Jan. 2018.
[35] M. Liu, D. Ma, and S. Li, "Neural dynamics for adaptive attitude tracking control of a flapping wing micro aerial vehicle," *Neurocomputing*, vol. 456, pp. 364–372, Oct. 2021.
[36] L. Jin, Y. Zhang, and B. Qiu, "Neural network-based discrete-time Z-type model of high accuracy in noisy environments for solving dynamic system of linear equations," *Neural Comput. Appl.*, vol. 29, no. 11, pp. 1217–1232, Jun. 2018.
[37] S. Wang, L. Jin, X. Du, and P. S. Stanimirovi, "Accelerated convergent zeroing neurodynamics models for solving multi-linear systems with M-tensors," *Neurocomputing*, vol. 458, pp. 271–283, Oct. 2021.
[38] Y. Zhang and Z. Ke, "On hyperbolic sine activation functions used in ZNN for time-varying matrix square roots finding," in *Proc. Int. Conf. Syst. Informat. (ICSAI)*, Yantai, China, May 2012, pp. 740–744.
[39] R. W. Coutinho, A. Boukerche, L. F. Vieira, and A. A. Loureiro, "Underwater wireless sensor networks: A new challenge for topology control-based systems," *ACM Comput. Surv.*, vol. 51, no. 1, pp. 1–36, 2018.
[40] H. Huang and Y. R. Zheng, "Node localization with AoA assistance in multi-hop underwater sensor networks," *Ad Hoc Netw.*, vol. 78, pp. 32–41, Sep. 2018.
[41] X. Du and Y. Su, *Research on Underwater Sensor Network*. Beijing, China: Science Press, 2016.
[42] L. Wang, X. Du, and C. Li, "FDR coding and decoding algorithm for reliable transmission in underwater acoustic network," *J. Commun.*, vol. 41, no. 4, pp. 81–91, Mar. 2020.

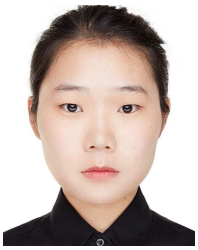

Lijuan Wang received the master's degree from Qinghai Normal University, Qinghai, China, in 2019, where she is now pursuing the Ph.D. degree. Her research interests include wireless sensor networks and neural networks.

Dan Su received the master's degree from the University of Texas at Austin, Austin, TX, USA, in 2017. She is currently pursuing the Ph.D. degree in artificial intelligence with the School of Information Science and Engineering, Lanzhou University, Lanzhou, China. Her research interests include neural networks, robotics, and intelligent information processing.

Mei Liu received the master's degree from Sun Yat-sen University, Guangzhou, China, in 2014. She is currently a Teacher with the School of Information Science and Engineering, Lanzhou University, Lanzhou, China. Her research interests include neural networks, computation, and optimization.

Xiujuan Du received the Ph.D. degree from Tianjin University, Tianjin, China, in 2010. She is currently a Professor with Qinghai Normal University, Qinghai, China. Her research interests include underwater acoustic networks, wireless network and security, and the Internet of Things. She has received the New Century Excellent Talent from Education Ministry, China, in 2011.